Bio-inspired Models of Memory Capacity, Recall Performance and Theta Phase Precession in the Hippocampus

Vassilis Cutsuridis, Bruce P. Graham, Stuart Cobb, and Michael E. Hasselmo

Abstract— **The hippocampus plays an important role in the encoding and retrieval of spatial and non-spatial memories. Much is known about the anatomical, physiological and molecular characteristics as well as the connectivity and synaptic properties of various cell types in the hippocampal circuits [1], but how these detailed properties of individual neurons give rise to the encoding and retrieval of memories remains unclear. Computational models play an instrumental role in providing clues on how these processes may take place. Here, we present three computational models of the region CA1 of the hippocampus at various levels of detail. Issues such as retrieval of memories as a function of cue loading, presentation frequency and learning paradigm, memory capacity, recall performance, and theta phase precession in the presence of dopamine neuromodulation and various types of inhibitory interneurons are addressed. The models lead to a number of experimentally testable predictions that may lead to a better understanding of the biophysical computations in the hippocampus.**

I. Introduction

The hippocampus is a key brain structure known to play a role in the encoding and retrieval of spatial (e.g. landmark) and non-spatial (e.g. object) memories. The principal excitatory cells (pyramidal cells (PCs)) exhibit firing patterns which code for spatial features (e.g. places) of the external world. The firing rate and phase of the pyramidal cells that code for place change with respect to theta oscillations [35]. Theta oscillations (4-10 Hz) are observed in rats during navigation and rapid eye movement (REM) sleep [29]. During exploration hippocampal place cells shift their phase of firing to earlier phases of the theta oscillation as the animal transverses the place field (a phenomenon known as theta phase precession) [35-36].

Network oscillations (theta, gamma, ripples) in the hippocampus are either internally generated [30] or are paced by extrahippocampal areas (e.g. medial septum (MS)) [42]. Theta oscillations have been suggested to contribute to memory formation [11] by separating the encoding of new information and the recall of old information in separate functional sub-cycles of theta. Gamma oscillations have been proposed to be an internal clock [34]. Ripples play a role in the replay of memories in a temporally compressed window [31-33].

In recent years a zoo of inhibitory interneurons has been identified in the hippocampus [24-28]. These cells are categorised based on their anatomical, morphological, pharmacological and physiological properties [23]. These include the axo-axonic cells (AAC), the perisomatic basket cells (BC) and the dendritic bistratified (BSC), ivy (IVY), neurogliaform (NGL) and oriens lacunosum-moleculare (OLM) cells [24], [26-27]. AACs target exclusively the axon of the CA1 PC, whereas BCs inhibit their cell bodies and proximal dendrites [24]. BSCs and IVYs inhibit the PC basal and oblique dendrites, whereas OLM and NGL cells target the apical dendritic tuft of PCs [24], [26-27].

Recent experimental studies have shown that the CA1 excitatory and inhibitory neurons fire at different phases of the theta oscillations [12-14, 41]. During theta, AACs, BCs and NGLs fire almost in phase with respect to the peak phases of theta, whereas BSCs, PCs, IVYs and OLM cells fire during the trough phases of theta [12-14, 41].

Similarly, medial septal (MS) GABAergic neurons differentially phase their activities with respect to theta oscillations [10], [15]. During theta, some MS GABAergic cells increase their firing during the peak of theta (MS_{180}), whereas others during the trough of theta (MS_{360}) [15].

As we speak further biological evidence is gathered from labs around the world on the properties of hippocampal cells with respect to theta, gamma and ripple oscillations. What we are trying to convey in this paper is that experimental evidence and detailed computational modeling have complementary roles in understanding the biophysical mechanisms and computations in the hippocampus. We show how such a marriage of theory and experiment within the context of encoding and retrieval of memory patterns in the hippocampus is possible in the next three sections.

II. Encoding and Retrieval of Memories as a Function of Cue Loading and Presentation Frequency

A. The Model

We've constructed a neural network model (see Fig. 1) of the region CA1 of the hippocampus consisting of 100 PCs, 2 BCs, 1 AAC, 1 BSC and 1 OLM cell [3-4], [6]. The cell numbers, morphology, ionic and synaptic properties, connectivity and spatial distribution followed closely the experimental evidence of the hippocampus [1]. All model

Manuscript received February 28, 2011. This work was supported by the EPSRC project grant EP/D04281X/1 and the NSF Science for Learning Center CELEST grant SMA 0835976.

V. Cutsuridis is with the Center for Memory and Brain, Boston University, Boston, MA 02215, USA (corresponding author; phone: 617-353-2840; fax: 617-358-3296; e-mail: vcut@bu.edu).

B.P. Graham is with the Institute of Computing Science and Mathematics, University of Stirling, U.K. (e-mail: b.graham@cs.stir.ac.uk).

S. Cobb is with the Institute of Neuroscience and Psychology, University of Glasgow, U.K. (e-mail: s.cobb@bio.gla.ac.uk).

M.E. Hasselmo is with the Center for Memory and Brain, Department of Psychology, and Graduate Program in Neuroscience, Boston University, Boston, MA 02215, USA (e-mail: hasselmo@bu.edu).

978-1-4244-9636-5/11/$26.00 ©2011 IEEE

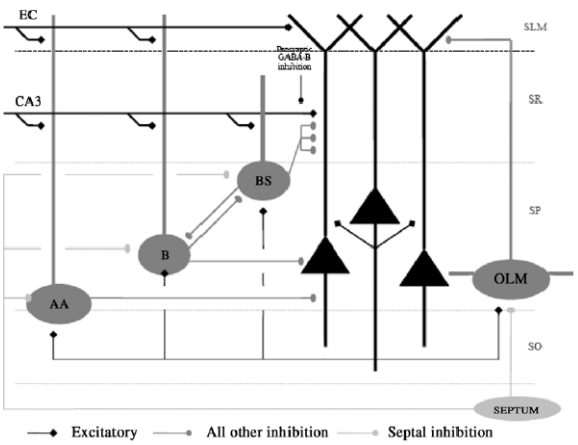

Fig. 1. Hippocampal CA1 microcircuit showing major cell types and their connectivity (adapted from [3] with permission). Black filled triangles: pyramidal cells. Dark gray filled circles: CA1 inhibitory interneurons. Light gray filled circles: Septal GABA inhibition. EC: entorhinal cortical input; CA3: CA3 Schaffer collateral input; AA: axo-axonic cell; B: basket cell; BS: bistratified cell; OLM: oriens lacunosum-moleculare cell; SLM: stratum lacunosum-moleculare; SR: stratum radiatum; SO: stratum oriens.

cell morphologies included a soma, an axon, and dendrites (proximal, distal and basal). The biophysical properties of each cell were adapted from cell types reported in the literature [16-19]. Dimensions of the somatic, axonic and dendritic compartments of the model cells were adapted from [37-38]. All passive and active ionic conductances, synaptic waveform parameters and synaptic conductances have been published elsewhere [5]. The complete Hodgkin-Huxley mathematical formalism of the model has been described in the appendix of [2] (see also [5]).

In the model, PCs were inhibited in the axon by the AAC, in the soma by the BCs, in the proximal dendrites by the BSC and the distal dendrites by the OLM cell, and in turn they excited all network INs in their basal dendrites. BC and BSC mutually inhibited each other, whereas the BC also inhibited the neighboring BC in the network. The OLM cell was excited by all PCs. All network INs were inhibited by GABAergic MS cells (MS_{180}).

AMPA, NMDA, GABA-A and GABA-B synapses were considered. GABA-A were present in soma, axon, proximal, distal and basal dendrites of cells, whereas AMPA and GABA-B were present only in the proximal and distal dendrites. NMDA synapses were present only in the proximal dendrites of the network PCs.

The strength of the CA3 Schaffer collateral input to the proximal PC dendrites was modulated by presynaptic GABA-B inhibition, which was active during the first half-cycle of theta and inactive during the second half-cycle of it.

PCs, BCs and AAC were excited in their distal dendrites by the entorhinal cortical (EC) input and in their proximal dendrites by the CA3 Schaffer collateral input. The BSC was only excited by the CA3 input.

Model EC and CA3 inputs were modeled as the firing of 20 entorhinal cortical cells and 20 out of 100 CA3 pyramidal cells. EC and CA3 inputs were presented every $\Delta\tau$ during the theta oscillation. $\Delta\tau$ was set to either 5ms, or 7ms, or 8ms or 10 ms or 11ms. EC inputs preceded the CA3 inputs by 9ms in accordance with experimental evidence that showed the conduction latency of the EC-layer III input to CA1 distal dendrites to range between 5 and 8 ms, whereas the conduction latency of the EC-layer II input to CA1 proximal dendrite via the trisynaptic loop to range between 12 and 18 ms [20-21].

A phenomenological spike timing-dependent plasticity (STDP) rule was used to modify the synaptic strength of the PC proximal AMPA synapses by comparing the CA3 input with the proximal postsynaptic voltage response. During recall, the PC proximal AMPA synaptic conductance was fixed and equated to the conductance value at the end of the encoding cycle plus a constant term, which represented the lift-off of the presynaptic GABA-B inhibition.

B. Simulation Results and Model Predictions

The model demonstrated the biological feasibility of the separation of encoding and retrieval processes into separate theta sub-cycles [11]. On the assumption that EC input always precedes the CA3 input by 9ms [20-21], the model predicted that the only way the EC and CA3 input patterns could be hetero-associated in the PC proximal dendrites is by maintaining an amplified postsynaptic voltage response for a sufficiently long period of time. The model predicted that such amplification of the PC proximal postsynaptic response *may* be due to the activation of, by the strong hyperpolarization from the BC and AAC inhibition of the soma and axon, non-specific cationic h-channels, which allowed the influx of Na^+ ions in the PC soma and proximal dendrites and hence the ``boosting'' of the proximal postsynaptic voltage response.

The model further predicted that the only way such careful timing can take place is if inhibitory cells are switched on and switched off in certain phase relationships with respect to the theta oscillation, as demonstrated by recent experimental data [12-14]. So, in the model, during storage the AACs and BCs were switched on and operated to: (1) exert tight inhibitory control on the axons and somas of the PCs, thus preventing them from firing during the storage cycle [12], (2) exert powerful inhibitory control to neighboring BCs and BSCs, preventing the latter from firing [13] during the encoding phase and disrupting the learning process, and (3) maintain the environment necessary for the activation of non-specific Na^+ -based cation h-channels and subsequently the amplification of the proximal postsynaptic response. During the retrieval phase, the septal inhibition was switched on, which in turn inhibited the AACs and BCs, which dis-inhibited the BSCs and allowed the PCs to fire action potentials and hence recall the information. BSCs provided a general broadcasting inhibitory signal to all PCs, which silenced all spurious cells in the network and allowed cells that have learnt the pattern to retrieve it. Finally, OLM cells were switched on during recall by the PC excitation [12-14] and inhibited the PC distal dendrites, thus preventing unwanted or similar memories from being retrieved.

The recall performance of the model (see Fig. 2) for a memory pattern was tested for different input pattern

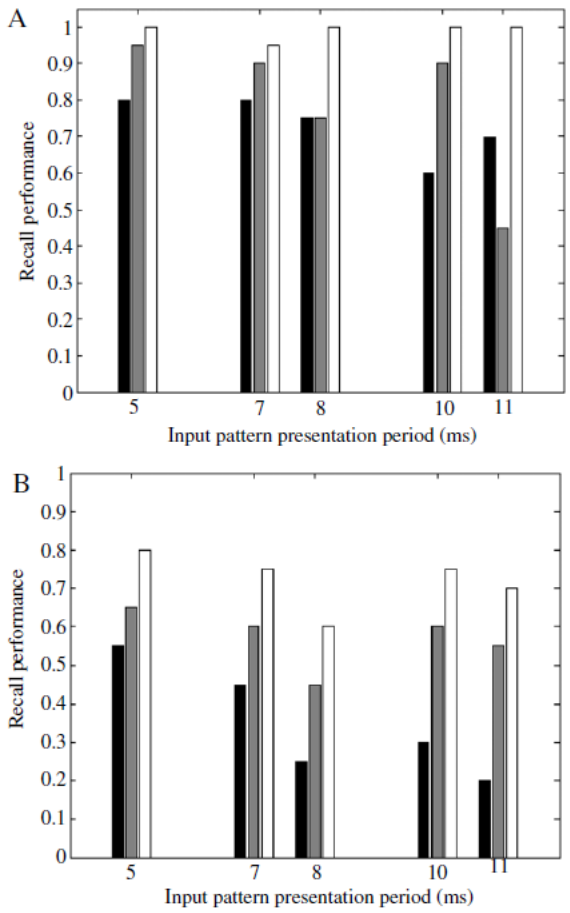

Fig. 2. Recall performance of pattern vector as a function of input pattern presentation period (adapted with permission from [3]). (A) Many-trials learning; (B) One-trial learning. *Black bar*: 10% cue loading; *Gray bar*: 50% cue loading; *White bar*: 75% cue loading.

presentation periods ($\Delta\tau$ = 5 ms, 7 ms, 8 ms, 10 ms and 11 ms), levels of cue (EC input) loading (10%, 50% and 75% of the cue was presented to PC) and learning paradigms (one-trial vs. many-trials). To estimate the recall performance, we counted the number of active cells in the pattern during a retrieval cycle and divided this number by the actual number of cells that ought to be active (pattern cells). If the active cells were equal to the pattern cells, then the recall fraction was 1 (i.e. perfect recall). At 75% cue loading, the recall performance for the "many-trials" case was nearly perfect (100%) regardless of the presentation period. At 50% and 10% cue loading in the "many-trials" case, the recall performance dropped by 5% and 20% respectively when the input presentation period was 5 ms. At larger input presentation periods, the recall performance degraded progressively for both 50% and 10% cue loading reaching a minimum of 45% and 70% respectively at 11 ms.

In the ``one-trial" case at 75% cue loading, the recall performance across input presentation periods varied slightly between 60% and 80%. At 50% and 10% cue loading, the recall performance dropped at 65% and 55% respectively at 5 ms. Across input presentation periods, the recall performance at 50% cue loading varied between 45% and 65%, whereas at 10% cue loading varied between 20% and 55%. Across learning case at 75% cue loading and 5ms time input presentation period, a drop of 20% in recall performance was observed between the "many-trial" and "one-trial" learning cases. Across all other presentation periods, the recall performance drop varied from 20% (7 ms) to 40% (8 ms) between the two cases. A constant 30% drop was observed across all presentation periods at 50% cue loading between the two cases with the exception of a 10% increase at 11 ms during the one-trial learning case. At 10% cue loading, the recall performance drop between the "many-trials" and the "one-trial" cases varied from 25% (5 ms) to 50% (8 ms and 11 ms).

III. TESTING MEMORY CAPACITY AND RECALL PERFORMANCE

A. The Model

We used the model of region CA1 of the hippocampus described in the previous section and changed it in the following ways in order to test its memory capacity and recall performance in the presence of various types of inhibitory interneurons. In contrast to the model described in the previous section, this model's EC and CA3 inputs were modeled as the firing of 20 entorhinal cortical cells and 20 out of 100 CA3 pyramidal cells, respectively, at an average gamma frequency of 40Hz. EC inputs preceded the CA3 inputs by 9ms in accordance with experimental evidence that showed the conduction latency of the EC-layer III input to CA1 apical dendrites to range between 5 and 8 ms, whereas the conduction latency of the EC-layer II input to CA1 basal dendrite via the trisynaptic loop to range between 12 and 18 ms [20-21].

All other parameters such as cell numbers, cell morphologies, passive and active ionic conductances, synaptic waveform parameters and synaptic conductances were left unchanged. The same phenomenological STDP rule as before was used here to modify the synaptic strength of the PC proximal AMPA synapses by comparing the relative timing between the CA3 input and the postsynaptic voltage response. During storage, the weights were initialized according to the predefined weight matrix and were allowed to change according to a clipped STDP rule. The low conductance state (gAMPA = 0.5 nS) was the minimum weight that could be achieved by long-term depression (LTD), whereas the high conductance state (gAMPA = 1.5 nS) was the saturated value that could be achieved by long-term potentiation (LTP). During each retrieval cycle the STDP learning rule was switched off. The conductance values from the last gamma cycle of the storage sub-cycle were used during the recall phase.

The recall performance metric used for measuring the distance between the recalled output pattern, C, from the required output pattern, C*, was the correlation (i.e., degree of overlap) metric, calculated as the normalized dot product:

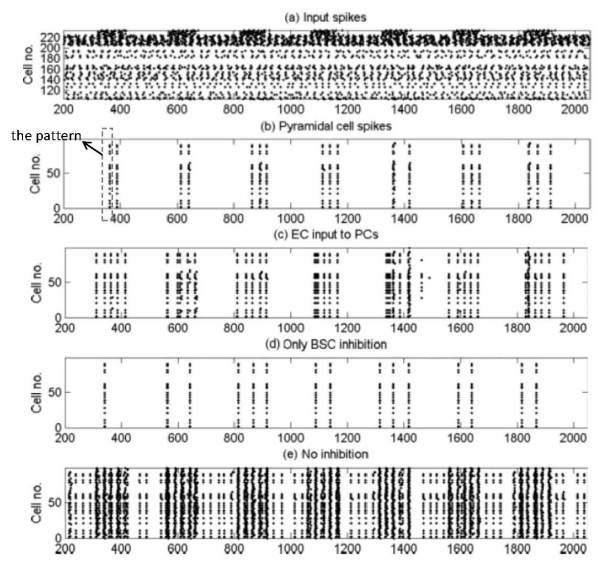

Fig. 3. Recall performance when recall is cued by the CA3 input (adapted from [2] with permission). Raster plots of (a) network inputs (b) PCs in full network (c) EC input now connected to PCs, so provides some recall cueing. (d) BC and AAC inhibition removed, so that recall is mediated only by BSC inhibition (EC disconnected from PCs). (e) BSC inhibition also removed. The *pattern recalled* was the firing activities of the cells activated by the EC input pattern.

$$R = C \cdot C^* / (\sum_{i=1}^{N_C} C_i \cdot \sum_{j=1}^{N_C} C_j^*)^{1/2} \qquad (1)$$

where N_C is the number of output units. The correlation takes a value between 0 (no correlation) and 1 (the vectors are identical). The higher the correlation, the better the recall performance.

B. Simulation Results and Model Predictions

We tested the recall performance of our network to an already stored set of patterns. This set of patterns was stored by generating a weight matrix based on a clipped Hebbian learning rule, and using the weight matrix to pre-specify the CA3 to CA1 PC connection weights. Each pattern consisted of 20 randomly chosen PCs out of the population of 100. The 100 by 100 dimensional weight matrix was created by setting matrix entry (i, j), $w_{ij} = 1$ if input PC i and output PC j were both active in the same pattern pair; otherwise weights were 0. The weight matrix was then applied to our network model by connecting a CA3 input to a CA1 PC with a high AMPA conductance (gAMPA = 1.5 nS) if their connection weight was 1, or with a low conductance (gAMPA = 0.5 nS) if their connection was 0.

To test recall of a previously stored pattern, the associated input pattern was applied as cue in the form of spiking of active CA3 inputs (the pattern) distributed within a gamma frequency time window (40 Hz). At the same time, the 20 EC inputs also fired randomly distributed within a 25 ms gamma window, while preceding the CA3 activity by 9ms. The recall of the first pattern in a set of five is shown in

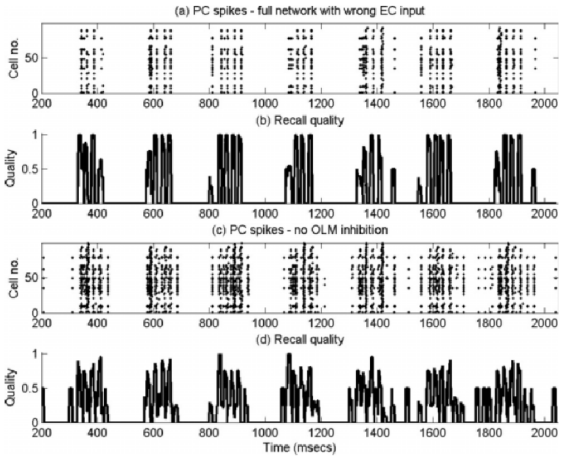

Fig. 4. Recall performance when recall is cued by the CA3 input, but EC input due to a different spurious pattern is present on PCs (adapted from [2] with permission). (a) Raster plot of PC activity in full network. (b) Recall quality in (a). (c) PC activity when OLM inhibition is removed. (d) Recall quality in (c).

Figure 3. Subplots (3a) and (3b) are raster plots of the spiking of (a) septal (top 10 rows), EC (next 20 rows) and CA3 (bottom 100 rows) input and (b) CA1 PCs when EC input is not present, respectively. The CA1 PCs are active two or three times during a recall cycle, with their spiking activity a very close match to the stored pattern. Subplot (3c) shows the PC recall performance when the EC input is present. The pattern is nearly perfectly recalled on each gamma cycle during a recall theta half-cycle.

We then tested the influence of the inhibitory pathways on recall by selectively removing different inhibitory pathways. In the model bistratified cell inhibition to proximal PC dendrites mediated thresholding of PC firing during recall. Removal of BC and AAC inhibition did not spoil recall quality in accord with this hypothesis (Fig. 3d). Removal of all inhibitory pathways led to gamma frequency firing of virtually all PCs during recall cycles and the EC cued pattern during recall cycles (Fig. 3e).

Recall performance was calculated by measuring the CA1

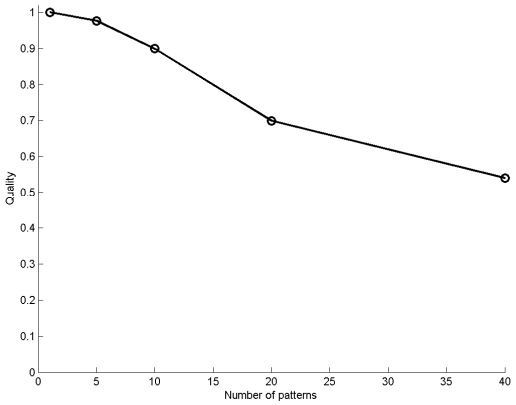

Fig. 5. Memory capacity of the CA1 microcircuit model (adapted from [2] with permission). Recall quality drops as the number of stored patterns increase.

PC spiking activity during a sliding 10 ms time window. For each window a binary vector of length 100 was formed, with entries having a value of 1 if the corresponding PC spikes in the window. The correlation of this vector with the expected pattern vector was calculated to give a measure of recall quality between 0 and 1, with 1 corresponding to perfect recall.

In the model OLM inhibition removed interference from spurious EC input during recall. Recall in this situation, with and without OLM inhibition to the SLM PC dendrites is shown in Figure 4. Recall was disrupted by the spurious EC input, but this disruption was significantly worse if the OLM inhibition is absent.

As was expected, average recall quality degraded when too many patterns were stored as PCs received more excitation from cue patterns they did not belong to, leading to spurious firing. Figure 5 shows the mean recall quality as the number of stored patterns is increased.

IV. THETA PHASE PRECESSION IN REGION CA1

A. The Model

We used the model of the CA1 microcircuit (see Fig 6) described in section III in order to investigate the roles different classes of the hippocampal and septal inhibitory interneurons play in the gating of the correct order of spatial memories in a sequence and the generation and maintenance of theta phase precession of pyramidal cells (place cells) in CA1 [7-9]. The present model was changed from the model in section III in the following ways: This reduced model consisted of four PCs, one BC, one BSC, one AAC and one OLM. Two additional types of inhibitory interneurons were also added to the current network: four IVY cells and four neurogliaform (NGL) cells. The IVYs inhibited the proximal dendrites of the PCs, whereas the NGLs inhibited the distal dendrites of the PCs. Each PC consisted of only four compartments (an axon, a soma, a proximal dendrite and a distal dendrite), whereas each IN consisted of a single compartment (soma).

In contrast to the model described in section III, PCs contained a fast Na^+ current, a delayed K^+ rectifier current, a low-voltage-activated (LVA) L-type Ca^{2+} current, an A-type K^+ current, and a calcium activated mAHP K^+ current. Active properties of BC, AAC, BSC and IVY included a fast Na^+, a delayed rectifier K^+, a leakage and a type-A K^+ currents [2], [7]. Active properties of the OLM cell included a fast Na^+ current, a delayed rectifier K^+ current, a persistent Na^+ current, a leakage current and an h-current [7], whereas those of the NGL cell included a fast Na^+ current, a delayed rectifier K^+ current and a leakage current.

In contrast to the previous model, each PC in the present model was inhibited in the axon by the AAC, in the soma by the BC, in proximal dendrite by the BSC and IVY cells, and in the distal dendrite by the NGL and OLM cells. Inhibitory interneurons were inhibited by MS_{180} and MS_{360} GABAergic cells, and which in turn inhibited the MS cells.

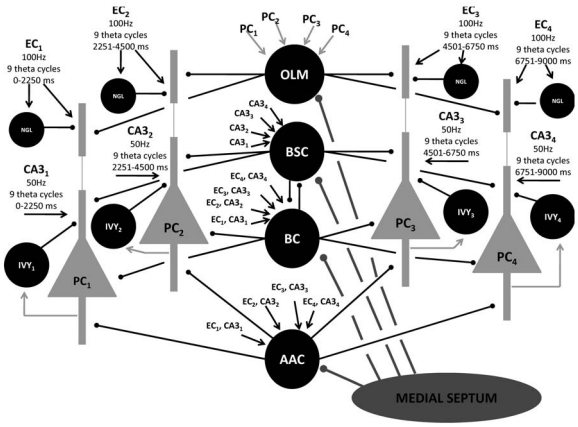

Fig. 6. Hippocampal CA1 microcircuit model showing major cell types and their connectivity (adapted from [8-9]). Black arrow lines: extra-hippocampal excitatory connections. Light gray arrow lines: PC excitatory connections to OLM cell. Black filled lines: CA1 inhibitory connections. Dark gray filled circles: septal inhibitory connections. EC: Layer III entorhinal cortical input. CA3: CA3 Schaffer collateral input. PC: pyramidal cell. AAC: axo-axonic cell. BC: basket cell. BSC: bistratified cell. OLM: oriens lacunosum-moleculare cell. NGL: neurogliaform cell. IVY: ivy cell. Note there is no recurrent connectivity between pyramidal cells in the circuit.

AMPA, NMDA, and GABA-A synapses were considered. AMPA and GABA-A were present in all compartments of INs and PCs. NMDA synapses were present both in proximal and distal dendrites of the PCs. Presynaptic GABA-B inhibition modulated the strength of the CA3 Schaffer collateral input to PC proximal synapses as before.

In contrast to the previous model, the EC and CA3 inputs arrived at the same time in the PC proximal dendrite. EC and CA3 inputs excited the AAC and the BC. BSC was excited only by the CA3 input, whereas NGL was excited only by the EC input. IVY and OLM cells were excited only by the PCs in the network. No other INs in the network received feedback excitation from the PCs.

Each pyramidal cell in the network received a different set of EC and CA3 inputs (PC_1 was excited by EC_1 and $CA3_1$, PC_2 by EC_2 and $CA3_2$, PC_3 by EC_3 and $CA3_3$ and PC_4 by EC_4 and $CA3_4$) (see Fig 6). The proper order by which the EC and CA3 inputs were presented to each PC (EC_1 and $CA3_1$ first, followed by EC_2 and $CA3_2$, then by EC_3 and $CA3_3$ and finally by EC_4 and CA_4) was ensured (gated) by dopamine in the distal layer. Dopamine acted as the *gate keeper* who opened the gate when a high frequency EC input impinged on both NGL and PC and closed the gate when a low frequency EC input impinged on both NGL and PC [39]. When the place cell was inside its place field, it received a high frequency (100Hz) input from EC. When the place cell was outside its place field, the frequency of the EC input was low (1-3 spikes per theta oscillation). The duration of each set of EC and CA3 inputs is 2250ms, which corresponded to nine theta cycles, each theta cycle with duration of 250ms. The presentation frequencies of the EC and CA3 inputs were set to 100Hz (interspike interval (ISI) = 10ms) and 50Hz (ISI = 20ms), respectively [40].

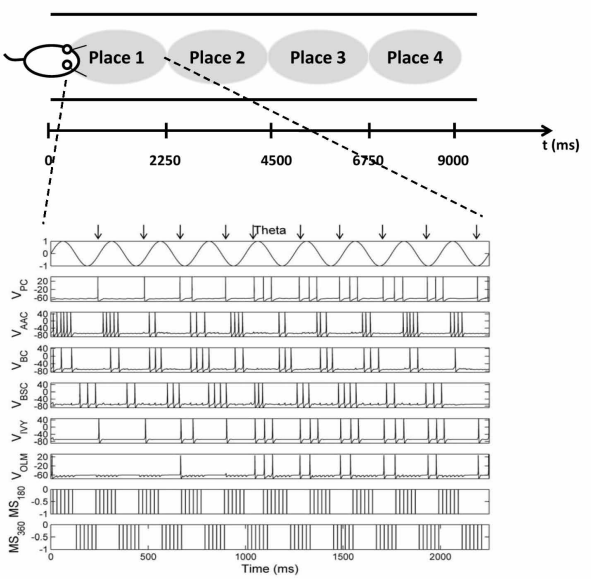

Fig. 7. (*Top*) A rat running along a linear track. Gray filled ellipses represent the place fields of four pyramidal cells (place cells) in the network. Note their fields are non-overlapping. The time the rat spends in each place field is equal to nine theta cycles, with each theta cycle lasting 250ms, a total time of 2250ms. As the rat transverses the place field, each PC shifts its firing to earlier phases of the theta rhythm. (*Bottom*) Spiking activity of CA1 and septal cells with respect to simulated theta oscillation as measured from the pyramidal layer of CA1 (adapted from [9]). Arrows indicate the phase the place cell fired with respect to theta.

In contrast to the phenomenological STDP rule used in model from section III, a biophysical STDP learning rule [22] was applied to both the proximal and distal NMDA synapses of the PCs in the present model. The mechanism had a modular structure consisting of three biochemical detectors: a potentiation (P) detector, a depression (D) detector and a veto (V) detector. Each detector responded to the instantaneous calcium level and its time course in the dendrite. The potentiation (P) detector triggered LTP every time the calcium levels were above a high-threshold (4μM). The depression (D) detector detected calcium levels exceeding a low threshold level (0.6μM). When the calcium levels remained above this threshold for a minimum time period, LTD was triggered. The veto (V) detector detected levels exceeding a mid-level threshold (2μM) and triggered a veto to the D response. P and D compete to influence the plasticity variable W, which serves as a measure of the sign and magnitude of synaptic strength changes from the baseline. In contrast to the previous models, the STDP learning rule was left on throughout all theta oscillations (i.e. weights were no longer fixed during the second half of theta).

B. Simulation Results and Model Predictions

Experimental studies have shown that place cells have specific properties when rats are inside the cell's place field: (1) all place cells start firing at the same initial phase [35]; (2) the initial phase is on average the same on each entry of the rat into the place field of a place cell [35]; (3) the total amount of phase precession is always less than 360° [35]; (4) the firing rate of the place cell increases as the position of the rat in the place field increases, reaching a maximal value at about 200° and beyond this point it decreases again.

The model, although it is not an explicit model of motion or direction of movement, was able to capture the observed properties of the place cells (see PC spiking activity with respect to theta oscillation in Fig. 7). The model predicted that in order for the place cells to phase precess to a full 360° as the rat reaches the end of the place field (ninth theta cycle), then an excitatory phase precessing CA3 input, should drive not only the PCs, but also the inhibitory interneurons causing them to also precess. An additional phase precessing inhibitory input (MS_{180} and MS_{360}), which inhibits the CA1 inhibitory interneurons, is also required to ensure that the phase relationships between the PCs and the inhibitory INs during theta are maintained, as has been observed experimentally [12-14].

Furthermore, the model predicted that in order for the place cells to increase and decrease their firing activity in a similar way to experimental data, then (1) a CA3 phase precessed input should drive both CA1 PCs and INs, and the frequency should linearly increase from the start till the middle of the place field and subsequently decrease linearly by the same amount till the end of the field, (2) a constant frequency phase precessed MS and presynaptic $GABA_B$ inhibition should also drive the CA1 INs and PCs, respectively, and (3) the PC proximal synapse should be slightly depressed.

V. CONCLUSIONS

Three computational models of the region CA1 of the hippocampus at various levels of biological detail have been presented. The models were successful at addressing issues such as retrieval of memories as a function of cue loading and presentation frequency in "one-trial" and "many-trials" learning schemes, memory capacity, recall performance and place cell firing rate and theta phase precession in the presence of neuromodulators (e.g. dopamine) and various classes of inhibitory interneurons. The models provided experimental testable clues of how encoding and retrieval of memories are achieved in the hippocampus and demonstrated how detailed computational models grounded on experimental data can provide clues on the types of computations performed in the hippocampus.

ACKNOWLEDGMENT

We would like to thank the two anonymous reviewers for their comments. This work was supported by the EPSRC project grant EP/D04281X/1 and the NSF Science for Learning Center CELEST grant SMA 0835976.

REFERENCES

[1] V. Cutsuridis, B.P. Graham, S. Cobb, I. Vida, *Hippocampal Microcircuits: A Computational Modeler's Resource Book*. Springer (USA), 2010.

[2] V. Cutsuridis, S. Cobb, and B.P. Graham,"Encoding and retrieval in the hippocampal CA1 microcircuit model",.*Hippocampus,* 20(3), pp. 423-446, 2010

[3] V. Cutsuridis, T. Wenneckers, "Hippocampus, microcircuits and associative memory", *Neural Networks,* 22(8), pp. 1120-8, 2009

[4] V. Cutsuridis, S. Cobb, B.P. Graham, "Encoding and Retrieval in a CA1 Microcircuit Model of the Hippocampus", *in Lecture Notes in Computer Science* , vol. 5164, V. Kurkova, et al., Eds. Springer-Verlag: Berlin Heidelberg, 2008, pp. 238–247

[5] B.P. Graham, V. Cutsuridis, R. Hunter, "Associative Memory Models of Hippocampal Areas CA1 and CA3", in *Hippocampal Microcircuits: A Computational Modeller's Resource Book,* V. Cutsuridis et al., Eds. Springer, USA, 2010, pp. 459-494

[6] B. P. Graham, and V. Cutsuridis, "Dynamical Information Processing in the CA1 Microcircuit of the Hippocampus", in *Computational Modeling in behavioral neuroscience: Closing the gap between neurophysiology and behavior*. D. Heinke, et al., Eds London: Psychology Press, Taylor and Francis Group, 2009, pp. 1- 31.

[7] V. Cutsuridis, and M. Hasselmo, "Dynamics and function of a CA1 model of the hippocampus during theta and ripples", in Lecture Notes in Computer Science, vol. 6352, K. Diamantaras, W. Duch, L.S. Iliadis, Eds., Springer-Verlag: Berlin Heidelberg, 2010, pp. 230-240.

[8] V. Cutsuridis, M. Hasselmo, "Spatial Memory Sequence Encoding and Replay during Modeled Theta and Ripple Oscillations", *accepted for publication*

[9] V. Cutsuridis, M. Hasselmo, "GABAergic modulation of gating, timing and theta phase precession of hippocampal neuronal activity during theta oscillations", u*nder review*

[10] G. Dragoi, D. Carpi, M. Recce, J. Csicsvari, and G. Buzsaki, "Interactions between hippocampus and medial septum during sharp waves and theta oscillation in the behaving rat", *J Neurosci*., 19(14), 1999, pp. 6191-99

[11] M. Hasselmo, C. Bodelon, and B. Wyble, "A proposed function of the hippocampal theta rhythm: separate phases of encoding and retrieval enhance reversal of prior learning", *Neural Comput*., 14, 2002, pp. 793-817

[12] T. Klausberger, P.J. Magill, L.F. Marton, J. David, B. Roberts, P.M. Cobden, G. Buzsaki, P. Somogyi, "Brain-state- and cell-type-specific firing of hippocampal interneurons in vivo", *Nature*, 421, 2003, pp. 844-848

[13] T. Klausberger, L.F. Marton, A. Baude, J.D. Roberts, P.J. Magill, P. Somogyi, "Spike timing of dendrite-targeting bistratified cells during hippocampal network oscillations in vivo", *Nat Neurosci.*, 7(1), 2004, pp. 41-7

[14] T. Klausberger and P. Somogyi, "Neuronal diversity and temporal dynamics: the unity of hippocampal circuit operations", *Science*, 321, 2008, pp. 53-57

[15] Z. Borhegyi, V. Varga, N. Szilagyi, D. Fabo, T.F. Freund, "Phase segregation of medial septal GABAergic neurons during hippocampal theta activity", *J Neurosci.*, 24(39), 2004, pp. 8470-79

[16] P. Poirazzi, T. Brannon, B.W. Mel, "Arithmetic of subthreshold synaptic summation in a model CA1 pyramidal cell", *Neuron*, 37, 2003a, pp. 977–987.

[17] P. Poirazzi, T. Brannon, B.W. Mel, "Pyramidal neuron as a 2-layer neural network", *Neuron*, 37, 2003b, pp. 989–999.

[18] V. Santhakumar, I. Aradi, I. Soltetz, "Role of mossy fiber sprouting and mossy cell loss in hyperexcitability: A network model of the dentate gyrus incorporating cells types and axonal topography", *J Neurophysiol*, 93, 2005, pp. 437–453

[19] F. Saraga, C.P. Wu, L. Zhang, F.K. Skinner, "Active dendrites and spike propagation in multicompartmental models of oriens-lacunosum/moleculare hippocampal interneurons", *J Physiol*., 552, 2003, pp. 673–689

[20] A.F. Soleng, M. Raastad, P. Andersen, "Conduction latency along CA3 hippocampal axons from rat", *Hippocampus*, 13, 2003, pp. 953–961

[21] L.S. Leung, L. Roth, K. J. Canning, "Entorhinal inputs to hippocampal CA1 and dentate gyrus in the rat: A current-source-density study", *J Neurophysiol*., 73, 1995, pp. 2392–2403

[22] J. E. Rubin, R. C. Gerkin, G. Q. Bi, C. C. Chow, "Calcium time course as signal for spike-timing-dependent plasticity", *J. Neurophysiol.,* 93, 2005, pp. 2600-2613

[23] G. A. Ascoli, L. Alonso-Nanclares, S. A. Anderson, G. Barionuevo, et al., "Petilla terminology: Nomenclature of features of GABAergic interneurons of the cerebral cortex", *Nat Rev Neurosci*, 9(7), 2008, pp. 557-568

[24] P. Somogyi, T. Klausberger, "Defined types of cortical interneurons structure space and spike timing in the hippocampus", *J Physiol.,* 562(1), 2005, pp. 9-26

[25] S. Jinno, T. Klausberger, L. F. Marton, Y. Dalezios, J. D. Roberts, P. Fuentealba, E. A. Bushong, D. Henze, G. Buzsáki, P. Somogyi, "Neuronal diversity in GABAergic long-range projections from the hippocampus", *J Neurosci.,* 27(33), 2007, pp. 8790-804

[26] P. Fuentealba, R. Begum, M. Capogna, S. Jinno, L. F. Márton, J. Csicsvari, A. Thomson, P. Somogyi, T. Klausberger, "Ivy cells: a population of nitric-oxide-producing, slow-spiking GABAergic neurons and their involvement in hippocampal network activity", *Neuron,* 57(6), 2008a, pp. 917-929

[27] P. Fuentealba, R. Tomioka, Y. Dalezios, L. F. Márton, M. Studet, K. Rockland, T. Klausberger, P. Somogyi, "Rhythmically active enkephalin-expressing GABAergic cells in the CA1 area of the hippocampus project to the subiculum and preferentially innervate interneurons", *J Neurosci.,* 28(40), 2008b, pp. 10017-22.

[28] C. R. Houser, "Interneurons of the dentate gyrus: An overview of cell types, terminal fields and neurochemical identity", *Progress in Brain Research*, 163, 2007, pp. 217-232.

[29] G. Buzsaki, " Theta oscillations in the hippocampus", *Neuron,* 33(3), 2002, pp. 325-40

[30] S.R. Cobb, E.H. Buhl, K. Halasy, O. Paulsen, P. Somogyi, "Synchronization of neuronal activity in hippocampus by individual GABAergic interneurons", *Nature*, 378(6552), 1995, pp. 75-8

[31] K. Diba, G. Buzsaki, "Forward and reverse hippocampal place-cell sequences during ripples", *Nat Neurosci.*, 10(10), 2007, pp. 1241-42

[32] D. J. Foster, M. A. Wilson, "Reverse replay of behavioural sequences in hippocampal place cells during the awake state", *Nature*, 440, 2006, pp. 680-83

[33] G. Dragoi, and S. Tonegawa, "Preplay of future place cell sequences by hippocampal cellular assemblies", Nature, 469, 2011, pp. 397-401

[34] B. P. Graham, (2003). "Dynamics of storage and recall in hippocampal associative memory networks", in *Computational neuroscience: cortical dynamics*, P. Erdi, A. Esposito, M. Marinaro, & S. Scarpetta Eds, Springer-Verlag: Berlin, Heidelberg, 2003, pp. 1–23

[35] J. O'Keefe, M. L. Recce, "Phase relationship between hippocampal place units and the EEG theta rhythm", *Hippocampus,* 3(3), 1993, pp. 317-330

[36] W. E. Skaggs, B. L. McNaughton, M. A. Wilson, C. A. Barnes, "Theta phase precession in hippocampal neuronal populations and the compression of temporal sequences", *Hippocampus,* 6, 1996, pp. 149-172

[37] A.I. Gulyas, M. Megias, Z. Emri, T.F. Freund, "Total number and ration of excitatory and inhibitory synapses converging onto single interneurons of different types in the CA1 area of the rat hippocampus", *J. Neurosci.,*. 19(22), 1999, pp. 10082-10097

[38] M. Megias, Z.S. Emri, T. F. Freund, A. I. Gulyas, "Total number and distribution of inhibitory and excitatory synapses on hippocampal CA1 pyramidal cells", *Neuroscience,* 102(3), 2001, pp. 527-40.

[39] H. T. Ito, E. M. Schuman, "Frequency-dependent gating of synaptic transmission and plasticity by dopamine", *Frontiers in Neural Circuits,* 1(1), 2007, pp. 1-13

[40] L.L. Colgin, T. Denninger, M. Fyhn, T. Hafting, T. Bonnevie, O. Jensen, M.B. Moser, E. I. Moser, "Frequency of gamma oscillations routes flow of information in the hippocampus", *Nature,* 462(19), 2009, pp. 353-358

[41] P. Fuentealba, T. Klausberger, T. Karayannis, W.Y. Suen, J. Huck, R. Tomioka, K. Rockland, M. Capogna, M. Studer, M. Morales, P. Somogyi, "Expression of COUP-TFII Nuclear Receptor in Restricted GABAergic Neuronal Populations in the Adult Rat Hippocampus", *J. Neurosci*. 30(5), 2010, pp. 1595-160

[42] K. Toth, Z. Borhegyi, T.F. Freund, ”Postsynaptic targets of GABAergic hippocampal neurons in the medial septum-diagonal band of Broca complex”, *J Neurosci,* 13, 1993, pp. 3712–3724